Eidgenössische
Technische Hochschule
Zürich

Ecole polytechnique fédérale de Zurich
Politecnico federale di Zurigo
Swiss Federal Institute of Technology Zurich

Exact Solver and Uniqueness Conditions for Riemann Problems of Ideal Magnetohydrodynamics

M. Torrilhon

Research Report No. 2002-06
April 2002

Seminar für Angewandte Mathematik
Eidgenössische Technische Hochschule
CH-8092 Zürich
Switzerland

Exact Solver and Uniqueness Conditions for Riemann Problems of Ideal Magnetohydrodynamics

M. Torrilhon

Seminar für Angewandte Mathematik
Eidgenössische Technische Hochschule
CH-8092 Zürich
Switzerland

Research Report No. 2002-06 April 2002

Abstract

This paper presents the technical details necessary to implement an exact solver for the Riemann problem of magnetohydrodynamics (MHD) and investigates the uniqueness of MHD Riemann solutions. The formulation of the solver results in a nonlinear algebraic 5×5 system of equations which has to be solved numerically.

The equations of MHD form a non-strict hyperbolic system with non-convex fluxfunction. Thus special care is needed for possible non-regular waves, like compound waves or overcompressive shocks. The structure of the Hugoniot loci will be demonstrated and the non-regularity discussed. Several non-regular *intermediate* waves could be taken into account inside the solver.

The non-strictness of the MHD system causes the Riemann problem also to be not unique. By virtue of the structure of the Hugoniot loci it follows, however, that the degree of freedom is reduced in the case of a non-regular solution. ¿From this, uniqueness conditions for the Riemann problem of MHD are deduced.

Keywords: hyperbolic systems of conservation laws, Riemann problem, magnetohydrodynamics, non-classical shocks

Subject Classification: 35-L45, 35-L67, 76-L05, 76-W05

1 Introduction

In a Riemann problem a system of hyperbolic equations in one space dimension

$$\partial_t u + \partial_x f(u) = 0 \qquad u \in \mathbb{R}^N \tag{1}$$

is furnished with discontinuous initial conditions in the form

$$u(x, t=0) = \begin{cases} u^{(1)} & x < 0 \\ u^{(0)} & x > 0 \end{cases} . \tag{2}$$

The solution of such problems is governed by the hyperbolic properties of the system (1). It is built from simple waves, either discontinuities, called shock waves, or rarefaction fans, which have to be assembled appropriately. The general procedure to solve Riemann problems may be found in textbooks like [14] or [19].

The equations of magnetohydrodynamics are formed from Euler equations of gasdynamics and the induction equation for the magnetic field. They describe the flow of a plasma in interaction with a magnetic field. The physics of the MHD system is described in [12], for example. Though the Euler equations are underlying, the hyperbolic properties of the MHD system are considerably more complex in comparison. There are not only more waves according to a larger system, in addition the system is non-strictly hyperbolic with non-convex fluxfunction and the characteristic fields are no longer either genuinely non-linear or linearly degenerated. By virtue of this, the MHD system may admit non-regular waves, like compound waves and overcompressive *intermediate* shocks.

These intermediate shocks had been abondoned by evolutionary arguments (see [11], [15]) in former times. The research of the last decade, however, showed that those waves seems to have physical significance. They may be formed numerically from steepening waves [20], are present in numerical calculations [3], [21], and even stable in 3d simulations under finite perturbations (see [4], [5]). In [8], [9] was shown that they posses a nonlinearly stable viscous profile in all cases. Thus they are conditionally stable in a nonlinear analysis (see also [16], [17]). Nevertheless, very recently it has been argued against non-evolutionary waves, like intermediate shocks, in [7]. Hence, the relevance of these waves is not yet completely clarified.

In this paper an exact Riemann solver for MHD is constructed. The construction results in a highly nonlinear 5×5 algebraic system of equations which is solved by Newtons method numerically. In order to give some insight into MHD Riemann problems, a solution example will be discussed in Section 2. The formulation of the solver (Section 3) will need the control of shocks (Section 4) and rarefaction waves (Section 5). Therefore, a detailed presentation of the MHD Hugoniot loci, which describe admissible shock waves, is given. Originally the evaluation of the MHD Rankine-Hugoniot-conditions has been done in [1] and [6]. This paper will collect results from these former papers and from textbooks ([11], [12] and [15]) in order to present a selfcontained describtion of the MHD Riemann solver. After the presentation of the Hugoniot loci the non-regular waves and their characteristic behavior is discussed. The implementation of the solver (Section 6) will admit some overcompressive shocks and compound waves to be inserted in the solution. Nevertheless not all intermediate shocks could be taken into account and it stays an open question how these waves come into play.

The solver is mainly developed to produce reliable solutions, which could be used as benchmarks for numerical methods. The investigations of numerical methods for MHD by using exact solutions obtained with the Riemann solver will be subject of a future paper.

The usage of the solver to calculate intercell fluxes inside a numerical method seems also to be interesting. However, due to the computational complexity of the exact solver, this is not worthwhile up to now.

Due to its non-convexity and non-strictness, the uniqueness of MHD Riemann problems is not assured by the theorem of Lax [13] (see also [18]). Indeed non-unique solutions are known [2] in which essentially regular waves are substituted by non-regular waves. The last section of this paper will investigate the uniqueness of MHD Riemann problems. The argumentation presented in that section will yield conditions on the initial data under which uniqueness of the solution is assured.

The details of the various formulas and calculations may be found in the appendixes of the paper.

2 MHD equations

The variables of ideal magnetohydrodynamics are the fields of density ρ, flow velocity $\mathbf{v}$, magnetic filed $\mathbf{B}$ and total energy E. In one-dimensional processes the vectorial variables $\mathbf{v}$ and $\mathbf{B}$ are splitted into their scalar normal components v_n and B_n in the direction of the space variable and the two-dimensional transversal parts $\mathbf{v}_t$ and $\mathbf{B}_t$. If x is the space direction, we have

$$\mathbf{B} = (B_x, B_y, B_z) = (B_n, \mathbf{B}_t) \quad \text{and} \quad \mathbf{v} = (v_x, v_y, v_z) = (v_n, \mathbf{v}_t)\,. \tag{3}$$

The absolute value of $\mathbf{B}_t$ will be denoted by

$$B_t = \|\mathbf{B}_t\|\,. \tag{4}$$

Due to the divergence condition which have to be imposed on the magnetic field, the normal component B_n have to be constant in space in one-dimensional processes. Throughout this paper the normal field B_n is assumed to be nonnegativ

$$B_n \geq 0. \tag{5}$$

The remaining seven fields

$$u = (\rho, v_n, \mathbf{v}_t, \mathbf{B}_t, E) \tag{6}$$

build the set of variables for one dimensional MHD. In this paper only ideal gases are considered and the total energy will be substituted by the pressure, which is related to E by

$$E = \frac{1}{\gamma - 1}p + \frac{1}{2}\rho v_n^2 + \frac{1}{2}\rho \mathbf{v}_t^2 + \frac{1}{2}\mathbf{B}_t^2. \tag{7}$$

Note, that in this equation the contribution of the normal field B_n is suppressed. In the numerical calculations of this paper the adiabaitic constant γ is set to be $\gamma = 5/3$.

The one dimensional MHD equations read

$$\begin{array}{lcll} \partial_t \rho & + & \partial_x \left(\rho v_n\right) & = 0 \\ \partial_t \rho v_n & + & \partial_x \left(\rho v_n^2 + p + \frac{1}{2}\mathbf{B}_t^2\right) & = 0 \\ \partial_t \rho \mathbf{v}_t & + & \partial_x \left(\rho v_n \mathbf{v}_t - B_n \mathbf{B}_t\right) & = 0 \\ \partial_t \mathbf{B}_t & + & \partial_x \left(v_n \mathbf{B}_t - B_n \mathbf{v}_t\right) & = 0 \\ \partial_t E & + & \partial_x \left(\left(E + p + \frac{1}{2}\mathbf{B}_t^2\right) v_n - B_n \mathbf{B}_t \cdot \mathbf{v}_t\right) & = 0 \end{array} \tag{8}$$

The equation for the normal component of the magnetic field reduces to the statement that B_n is also constant in time. The normal field B_n is thus considered only as parameter.

The system (8) is hyperbolic and has the characteristic velocites

$$\begin{aligned} &\lambda_1 = v - c_f,\ \lambda_2 = v - c_A,\ \lambda_3 = v - c_s, \\ &\lambda_4 = v, \\ &\lambda_5 = v + c_s,\ \lambda_6 = v + c_A,\ \lambda_7 = v + c_f, \end{aligned} \tag{9}$$

which are formed by the fast and slow magnetoacustic velocities $c_{f,s}$, and the Alfven velocity c_A, given by

$$c_{f,s} = \sqrt{\frac{1}{2}\left(\tfrac{B_n^2+B_t^2}{\rho} + a^2\right) \pm \sqrt{\frac{1}{4}\left(\tfrac{B_n^2+B_t^2}{\rho} + a^2\right)^2 - a^2\tfrac{B_n^2}{\rho}}} \tag{10}$$

$$c_A = \sqrt{\tfrac{B_n^2}{\rho}}. \tag{11}$$

Here the usual sound speed of gas dynamics $a = \sqrt{\gamma \frac{p}{\rho}}$ is used as abreviation. Since

$$c_s \leq c_A \leq c_f \tag{12}$$

the eigenvalues may coinside at special points in the flow. Hence, the system (8) is only *non-strictly* hyberbolic.

In the regular case, the solution of a Riemann problem (2) for the MHD system is governed by seven waves, either discontinuities or rarefaction fans. Each wave is associated to a characteristic velocity in the following way

$$v \pm c_f : \quad \text{fast shock/rarefaction to the right/left} \tag{13}$$

$$v \pm c_A : \quad \text{rotational discontinuity to the right/left} \tag{14}$$

$$v \pm c_s : \quad \text{slow shock/rarfaction to the right/left} \tag{15}$$

$$v : \quad \text{contact discontinuity} \tag{16}$$

The contact and rotational discontinuities are linear waves.

2.1 Example of a Riemann problem

Befor the actual Riemann solver is formulated, it is instructive to present a solution as an example. This will increase the understanding of the following sections.

As mentioned above the normal magnetic field B_n has to be constant

$$B_n^{(0)} = B_n^{(1)} = B_n, \tag{17}$$

and will be prescribed only as parameter additionally to the initial conditions (2). The transversal field $\mathbf{B}_t$, however, may vary from state 0 to state 1. In Fig. 1 general initial conditions for the magnetic field are shown. The absolute value as well as the direction of $\mathbf{B}_t$ may be different in both halfspaces. The initial twist angle of the planes of the magnetic fields is denoted by α. In the case of $\alpha = 0$ the Riemann problem is called planar, whereas the case $\alpha = \pi$ is called *co-planar*.

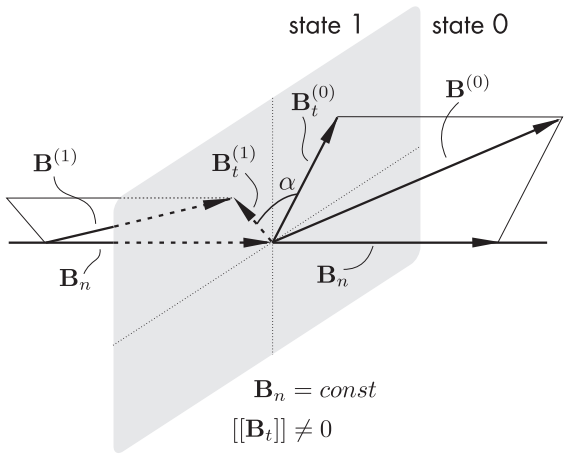

Figure 1: The initial conditions of a Riemann problem are separated into the constant states 0 and 1. Due to the divergence constraint the normal component of the magnetic field is not allowed to differ in both states. The transversal part may have different absolute values as well as a twist angle α. The same setting is used in the evaluation of the Rankine-Hugoniot-conditions in Sec. 4.

As example let us look at initial conditions given by

$$\left(\rho_1, v_n^{(1)}, \mathbf{v}_t^{(1)}, B_n, \mathbf{B}_t^{(1)}, p_1\right) = \left(3, 0, \mathbf{0}, \frac{3}{2}, \begin{pmatrix} 1 \\ 0 \end{pmatrix}, 3\right) \tag{18}$$

$$\left(\rho_0, v_n^{(0)}, \mathbf{v}_t^{(0)}, B_n, \mathbf{B}_t^{(0)}, p_0\right) = \left(1, 0, \mathbf{0}, \frac{3}{2}, \begin{pmatrix} \cos\alpha \\ \sin\alpha \end{pmatrix}, 1\right) \tag{19}$$

with twist angle $\alpha = 1/2$, so the initial transversal components of the magnetic field are twisted by almost 90 degrees. The pressure and density fields are chosen analogously to standard shocktube problems of ordinary gas dynamics.

In Fig. 2 the solution of (18)/(19) is depicted at time $t = 0.4$. Additional to the set of variables (6) the temperature $T \sim p/\rho$ is shown in the upper right corner. As you can read off the figure, none of the fields exhibits *all* seven MHD waves. The contact is only visible in the field of the density (and of the temperature). The rotations change only the transversal magnetic field and the transversal velocity. The fast and slow waves may be identified in each field: To the left there are a fast and slow rarefaction wave and to the right a fast and a slow shock. The exclusive appearence of rarefactions to the left and shocks to the right is a coincidence.

More insight into the behavior of the magnetic field is obtained by displaying the solution for $\mathbf{B}_t$ in the (B_y, B_z)-plane. This is done in Fig. 3. The solution forms a polygon whose legs represent the different waves. From the figure one main property of MHD Riemann problems may be extracted. The fast and the slow waves change only the absolute value of the transversal magnetic field. The rotational waves, in contrast, only rotate the transversal field. The exact solution, of course, gives only the left and right states of a rotation. The arcs in Fig. 3 are added to guide the eye.

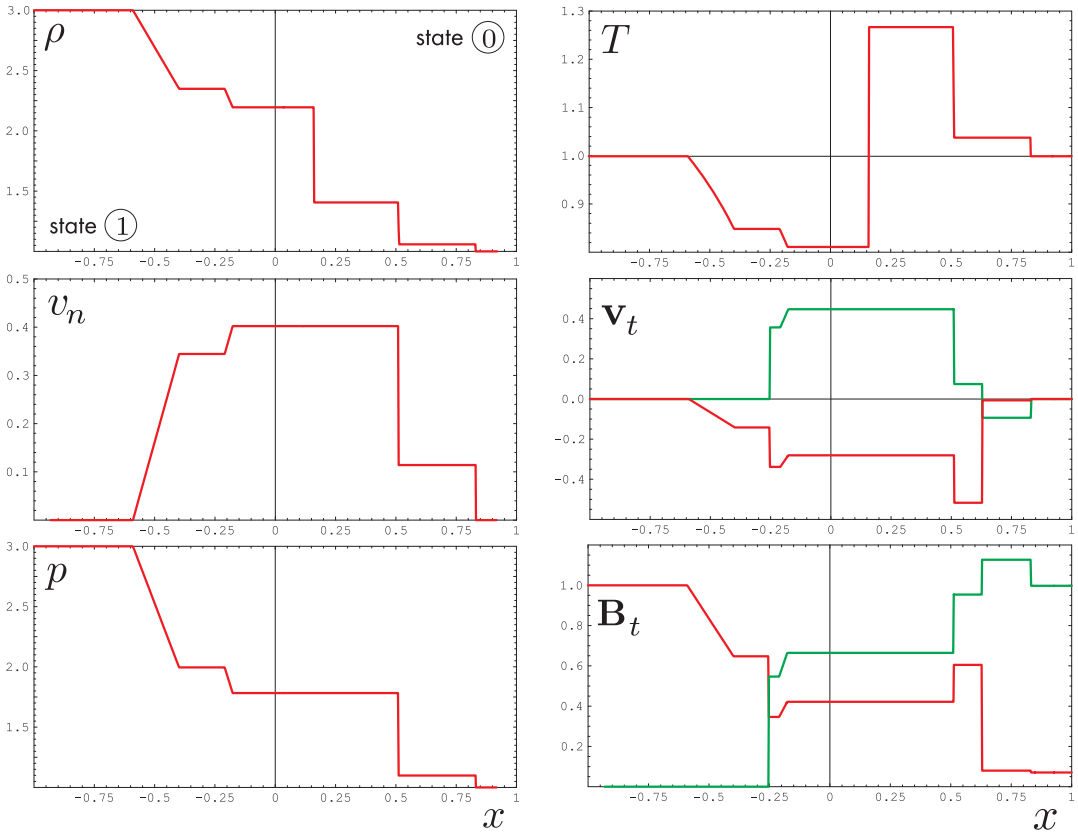

Figure 2: The solution of the Riemann problem with initial conditions (18)/(19) at time $t = 0.4$. The fields of density ρ, normal velocity v_n, pressure p, temperature T as well as transversal components of the velocity and of the magnetic field are shown.

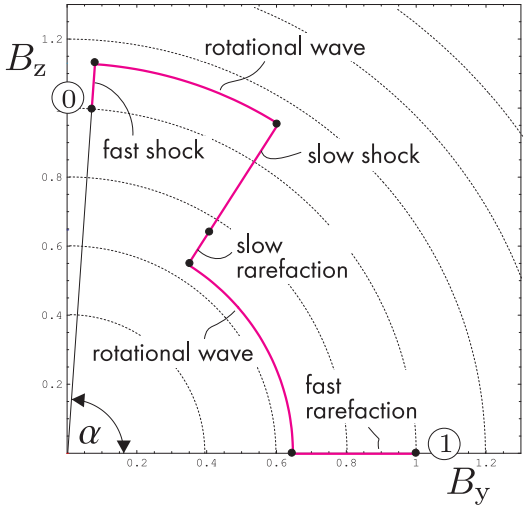

Figure 3: Solution of the Riemann problem (18)/(19) for the transversal magnetic field shown in the (B_y, B_z)-plane. In the waves occuring in the MHD Riemann problem either only the absolute value or only the direction of $\mathbf{B}_t$ is changed.

3 Formulation of the solver

Any wave in a Riemann problem is controlled by a single parameter, a pathvariable ψ. Given the fields in front of the wave, the fields behind are functions of this parameter. In order to solve the Riemann problem one has to find the parameter of each wave such that the initial conditions

$$U = (\mathbf{u}_0, \mathbf{u}_1) \tag{20}$$

are met beyond the fastest waves to the left and the right. This leads to a nonlinear algebraic system

$$\mathrm{RP}_U(\Psi) = 0, \tag{21}$$

which have to be solved for the vector of the pathvariables Ψ. The vectorvalued function RP_U calculates the residuum by comparison with the initial conditions U. The MHD Riemann problem consists of seven waves and seven fields, but (21) may be reduced to be a 5×5 system.

Firstly, both rotational discontinuities are described by specification of only one angle α_R. This follows from the fact that only these waves twist $\mathbf{B}_t$. If the initial twist angle and one rotation is given, the other roation angle $\alpha_R^\star$ may be calculated via $\alpha_R^\star = \alpha - \alpha_R$. Hence, by the angle α_R and the initial conditions, the direction of $\mathbf{B}_t$ is prescribed and only the absolute value B_t need additional considerations.

Secondly, the contact discontinuity may be eliminated by considering the left and the right part of the solution separately. This is also done when solving the Riemann problem for Euler equations. In this procedure the right/left waves are inserted starting from the right/left part of the initial conditions and the residuum is calculated at the contact discontinuity. At this point all fields are continuous, except the density field, which needs not to be considered.

Formally we write

$$(p^\star, v_n^\star, \mathbf{v}_t^\star, B_t^\star) = \mathrm{RP}_{\mathbf{u}}^\star(\psi_{s,f}, \alpha) \tag{22}$$

for the calculation of one half of the Riemann problem. The function $\mathrm{RP}_{\mathbf{u}}^*(\psi_{s,f}, \alpha)$ starts from the fields given by $\mathbf{u}$ and calculates the values of the fields after inserting fast/slow wave with parameter $\psi_{s,f}$ and a rotation with angle α. With respect to the residuum only the five fields of pressure p, of velocity $(v_n, \mathbf{v}_t)$ and the absolute value of the transversal magnetic field B_t are used.

The nonlinear system of (21) now has the form

$$\mathrm{RP}_U(\Psi) := \mathrm{RP}_{\mathbf{u}_0}^\star\left(\psi_{s,f}^-, \alpha_R\right) - \mathrm{RP}_{\mathbf{u}_1}^\star\left(\psi_{s,f}^+, \alpha - \alpha_R\right) = 0 \in \mathbb{R}^5 \tag{23}$$

with the vector

$$\Psi = \left(\psi_{s,f}^\pm, \alpha_R\right) \in \mathbb{R}^5. \tag{24}$$

The pathvariables $\psi_{s,f}^\pm$ are associated with the left and right going fast and slow waves and the angle α_R describes both rotations.

4 Controlling the discontinuities

The pathvariables which control the discontinuities usually come from a parametrization of the Hugoniot locus. The Hugoniot locus is build out of the solutions of the jump

conditions, or Rankine-Hugoniot-conditions, which read

$$s\left[\left[u\right]\right] - \left[\left[f\left(u\right)\right]\right] = 0 \tag{25}$$

for the general system (1). The quantity

$$\left[\left[\varphi\right]\right] := \varphi^{(1)} - \varphi^{(0)} \tag{26}$$

describes the jump of the fields to right and left of the discontinuity. The propagation velocity of the discontinuity is denoted by s. The Hugoniot locus is now given by

$$H_i\left(\psi; u^{(0)}\right) = \left\{u_i^{(1)}\left(\psi\right) \mid s_i\left(\psi\right)\left(u_i^{(1)}\left(\psi\right) - u^{(0)}\right) = f(u_i^{(1)}\left(\psi\right)) - f(u^{(0)})\right\}. \tag{27}$$

The index i represents the wave family to which the solution $u^{(1)}$ is associated, i.e. fast, slow or rotational. A solution is said to be associated to the family i, if

$$u_i^{(1)}\left(\psi \to \psi_0\right) \to u^{(0)} \quad \Rightarrow \quad s_i\left(\psi_0\right) = \lambda_i \tag{28}$$

holds. That is, a infinitesimal wave travels with the corresponding characteristic velocity. By virtue of this definition, each solution of (25) may be identified to belong to a certain family. We will see, that the choice $\psi = s$, i.e. using the shock speed as pathvariable, is possible only for fast shocks.

The Rankine-Hugoniot-conditions are evaluated most conveniently in a Galilei-transformed frame in which the discontinuity remains stationary. In such a frame (25) reduces to

$$\left[\left[f\left(u\right)\right]\right] = 0. \tag{29}$$

If one defines by $m := \rho v_n$ the mass flux, from (29) and $(8)_1$ follows

$$m = const. \tag{30}$$

The other equations of (8) inserted in (29) give after some calculations

$$\begin{array}{rcl} m^2\left[\left[v\right]\right] + \left[\left[p + \frac{1}{2}\mathbf{B}_t^2\right]\right] & = & 0 \\ m\left[\left[\mathbf{v}_t\right]\right] - B_n\left[\left[\mathbf{B}_t\right]\right] & = & 0 \\ m\left[\left[v\mathbf{B}_t\right]\right] - B_n\left[\left[\mathbf{v}_t\right]\right] & = & 0 \\ \left[\left[\frac{\gamma}{\gamma-1}pv + \frac{1}{2}m^2v^2 + \left(v - \frac{B_n^2}{2\,m^2}\right)\mathbf{B}_t^2\right]\right] & = & 0 \end{array} \tag{31}$$

where the specific volume

$$v := \frac{1}{\rho} \tag{32}$$

replaced the density.

To calculate the Hugoniot locus one has to proceed in principle as follows: Let the 0-state

$$\left(\rho_0, \mathbf{v}_t^{(0)}, \mathbf{B}_t^{(0)}, p_0\right) \tag{33}$$

be given together with B_n as parameter. Then choose the speed of propagation $v_n^{(0)} = s$ and thus m and calculate the 1-state variables

$$\left(\rho_1, \mathbf{v}_t^{(1)}, \mathbf{B}_t^{(1)}, p_1\right) \tag{34}$$

from (31). The normal velocity of state 1 is given by

$$v_n^{(1)} = \frac{\rho_0}{\rho_1} v_n^{(0)} \tag{35}$$

modulo Galilei invariance.

A shock wave is physically admissibe only if the entropy is increased through the shock. In magnetohydrodynamics the entropy η has the same form as in ordinary gasdynamics

$$\eta\,(p,\rho) = \ln \frac{p}{\rho^\gamma} \tag{36}$$

and it can be shown (e.g. [12]) that for a shockwave the condition $\eta_1 > \eta_0$ is equivalent to

$$\rho_1 > \rho_0. \tag{37}$$

Hence, like in the case of Euler equation only compression is allowed in a shock. In the Hugoniot loci presented below the expansion parts have been neglected.

4.1 Rotational wave

The rotational discontinuity is a linear wave with

$$[[v]] = 0 \quad [[p]] = 0 \quad \left[\left[\mathbf{B}_t^2\right]\right] = 0. \tag{38}$$

¿From this follows m out of (31) and

$$v_n^{(1)} = v_n^{(0)} = \frac{B_n}{\sqrt{\rho_0}} = \frac{B_n}{\sqrt{\rho_1}} \tag{39}$$

As expected from the linear degeneracy, any rotational discontinuity travels with the Alfven velocity. As pathvariable the change of the direction of $\mathbf{B}_t$ is most appropiate. Since the absolute value is preserved, the jump $[[\mathbf{B}_t]]$ may be calculated by the angle α_R and then the transversal velocity follows from $(31)_2$

$$[[\mathbf{v}_t]] = \pm \frac{1}{\sqrt{\rho}} [[\mathbf{B}_t]]\,. \tag{40}$$

The +-sign (−-sign) belongs to a left (right) travelling wave.

4.2 Shocks

If the jump of the density, respectively of the specific volume is nonzero, $[[v]] \neq 0$, the resulting discontinuity is called a shock. It may be deduced from $(31)_3$ that the transversal magnetic fields at both sides of any shock are collinear. Thus only the absolute value of $\mathbf{B}_t$ needs to be considered across a shock wave, which will be allowed to become negative.

By eliminating the transversal velocity between $(31)_2$ and $(31)_3$ and after some rearrangements, the Rankine-Hugoniot-conditions for a shock may be written as

$$\begin{array}{rcl} m^2\,[[v]] + [[p]] + \frac{1}{2}\left[\left[B_t^2\right]\right] & = & 0 \\ m^2\,[[vB_t]] - B_n^2\,[[B_t]] & = & 0 \\ \frac{1}{\gamma-1}\,[[pv]] + \frac{1}{2}\,(p_0+p_1)\,[[v]] + \frac{1}{4}\,[[v]]\,[[B_t]]^{\,2} & = & 0 \end{array} \tag{41}$$

It is now usefull to define dimensionless quantities by

$$\hat{v} = \frac{v_1}{v_0} \qquad \hat{p} = \frac{p_1}{p_0} \qquad \hat{B}_t = \frac{B_t^{(1)}}{\sqrt{p_0}} \qquad \hat{\mathbf{v}}_t = \frac{\mathbf{v}_t}{a_0}. \tag{42}$$

It is quite common to scale pressure and transversal field by the normal field B_n, but the definitions (42) cause less trouble if $B_n \to 0$. The Rankine-Hugoniot-conditions (41) then read

$$\begin{aligned} \hat{p} - 1 + \gamma M_0^2 (\hat{v} - 1) + \tfrac{1}{2}\left(\hat{B}_t^2 - A^2\right) &= 0 \\ \gamma M_0^2 \left(\hat{v}\hat{B}_t - A\right) - B^2\left(\hat{B}_t - A\right) &= 0 \\ \tfrac{1}{\gamma-1}(\hat{p}\hat{v} - 1) + \tfrac{1}{2}(\hat{v} - 1)(\hat{p} + 1) + \tfrac{1}{4}(\hat{v} - 1)\left(\hat{B}_t - A\right)^2 &= 0 \end{aligned} \tag{43}$$

with the three parameters

$$A = \frac{B_t^{(0)}}{\sqrt{p_0}} \qquad B = \frac{B_n}{\sqrt{p_0}} \qquad M_0 = \frac{v_n|_0}{a_0} = \frac{m}{\sqrt{\gamma p_0/v_0}}. \tag{44}$$

The parameters A and B describe the magnetic field in front of the shock and the Mach number M_0 is the shock speed scaled by the gasdynamical speed of sound.

In dimensionless variables the state 0 is given by

$$\left(\hat{v}, \hat{B}_t, \hat{p}\right)\Big|_0 = (1, A, 1) \tag{45}$$

and the variables $(\hat{v}, \hat{B}_t, \hat{p})\Big|_1$ at state 1 may be calculated from (43) after fixing the parameters A, B and M_0. Once this is done, the remaining variables follow from

$$\hat{v}_n|_1 = \frac{1}{\hat{\rho}}\,\hat{v}_n|_0 \qquad [[\hat{\mathbf{v}}_t]] = \pm\frac{\hat{B}}{\gamma M_0}\left[\left[\hat{\mathbf{B}}_t\right]\right], \tag{46}$$

where again the +-sign (−-sign) belongs to a left (right) travelling wave.

4.2.1 Fast Hugoniot locus

If the propagation speed approaches the fast magnetoacustic velocity, i.e.

$$M_0 \to \hat{c}_f^{(0)}(A, B) = \frac{c_f|_0}{a_0}, \tag{47}$$

a fast shock arises. It turned out by numerical evaluation, that the shock speed, resp. M_0, is indeed a practical pathvariable, since it varies monotonically along the fast Hugoniot locus. The calculation of the fields in the case $A \neq 0$, $B \neq 0$ is done by solving a cubic equation numerically, which is deduced from the system (43). In the cases $A = 0$ and $B = 0$ analytic expressions are available. Detailed formulas are presented in Appendix A.

In Fig. 4 the values of transversal magnetic field, pressure and specific volume along the fast Hugoniot curve are shown. The different curves referr to different choices of the parameters A and B. At the left hand side A (and thus $B_t^{(0)}$) is constant and B (resp. B_n) takes increasing values and vice versa at the right hand side. The figure should be read as follows: Suppose the values of the fields in front of a shock are given. This fixes a certain curve in the diagram for the transversal field, the pressure and the specific volume. Then

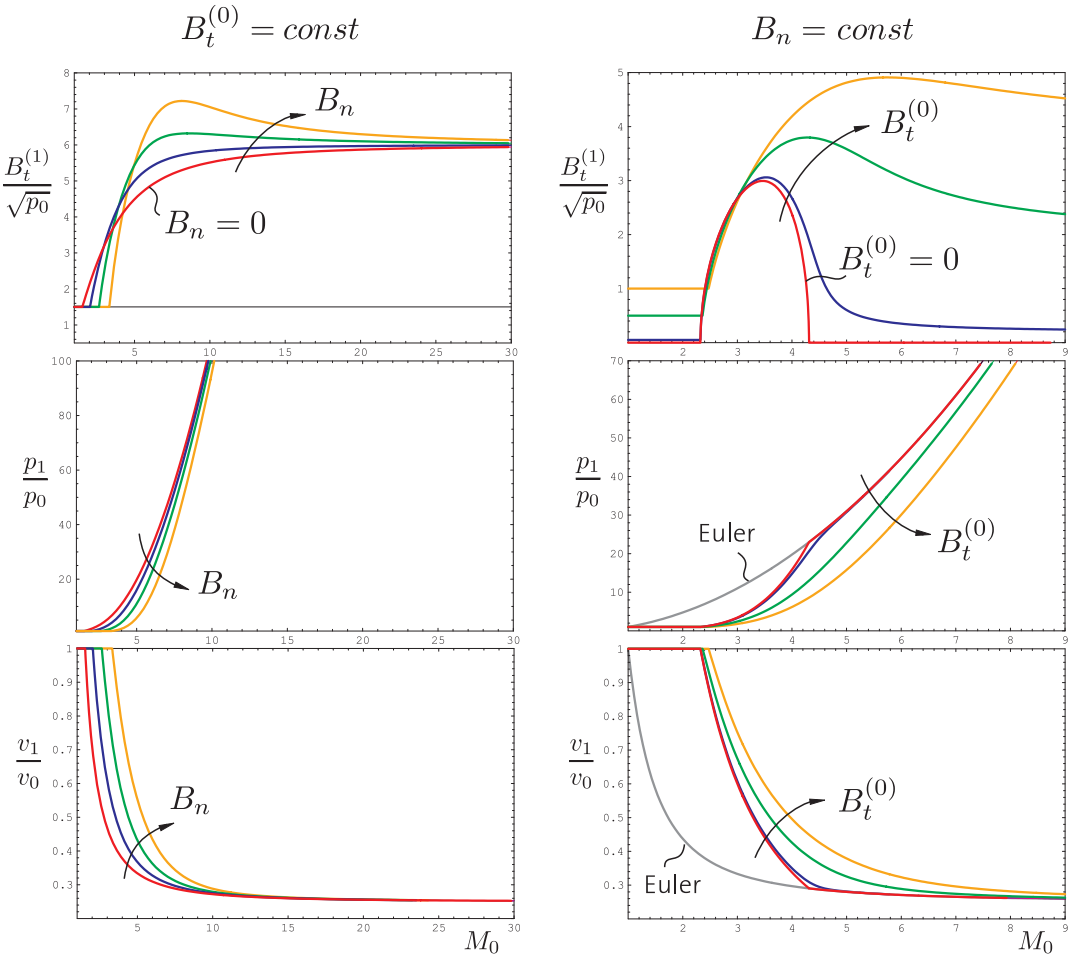

Figure 4: Hugoniot locus of the fast characteristic family in MHD. Behavior of transversal magnetic field, pressure and specific volume are plotted versus Mach number of the resulting shock wave. At the left hand side Hugoniot loci for different values of the normal magnetic field are shown ($A = 1.5 \;\; / \;\; B = 0, 2, 3, 4$), whereas at the right hand side the initial transversal field varies between the different curves ($B = 3 \;\; / \;\; A = 0, 0.05, 0.5, 1$).

choose a Mach number at the abscissae as propagation speed of the shock. The values of the fields behind the shock may now be found at the corresponding ordinates.

The decrease of the specific volume is limited by

$$v \underset{M_0 \to \infty}{\longrightarrow} \frac{\gamma-1}{\gamma+1} \tag{48}$$

in a fast shock. This behavior is known from the Euler equations. The transversal magnetic field along the Hugoniot locus has the asymptote

$$B_t \underset{M_0 \to \infty}{\longrightarrow} \frac{\gamma+1}{\gamma-1} A, \tag{49}$$

what follows from $(43)_2$. Nevertheless, for B large enough, higher values of B_t behind a fast shock are possible since the graph becomes non-monotone.

At the right hand side we see the Hugoniot curve for $A = 0$, i.e. for vanishing transversal

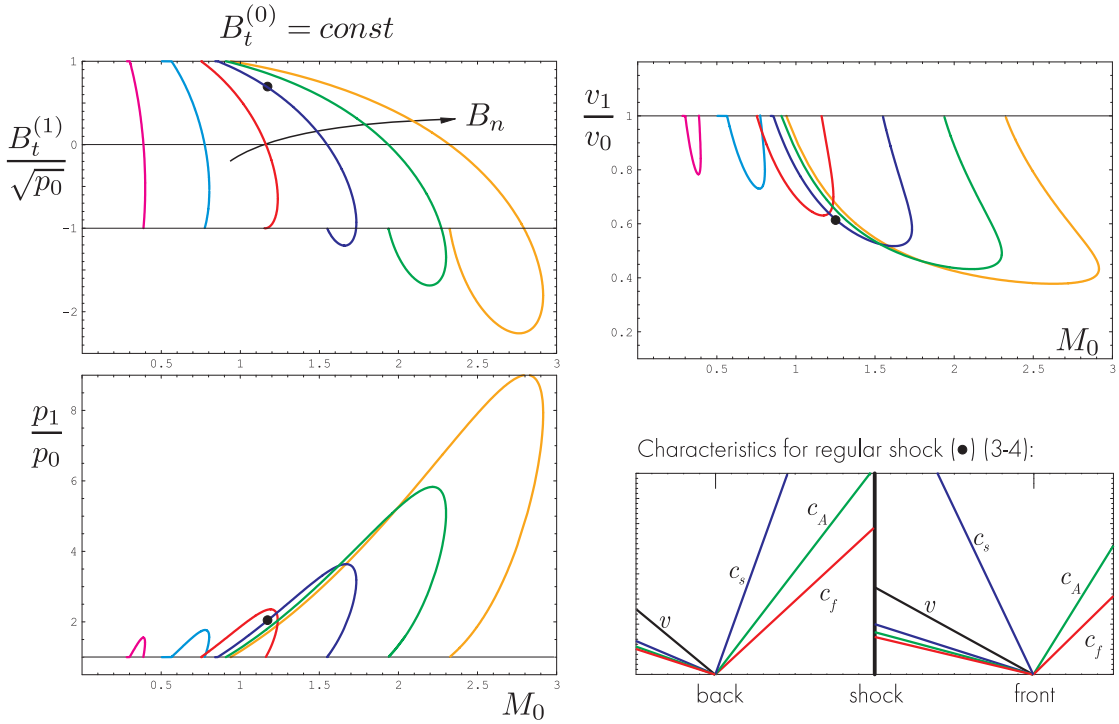

Figure 5: Hugoniot locus of the slow characteristic family of MHD for different values of the normal magnetic field ($A = 1 \quad / \quad B = 0.5, 1, 1.5, 2, 2.5, 3$). Behavior of transversal magnetic field, pressure and specific volume versus Mach number of the resulting shock. Additionally, in the lower right corner the characteristic curves in front and in the back of a regular slow shock are sketched.

magnetic field in front of the shock. Within the interval

$$\hat{c}_f^{(0)}(0, B) < M_0 < \sqrt{\frac{\gamma+1}{\gamma-1}\frac{B^2}{\gamma} - \frac{2}{\gamma-1}} \tag{50}$$

the transversal magnetic field behind the shock does not vanish indicating the existence of a "switch-on" shock. This interval is only non-empty if $B^2 > \gamma$. Beyond the interval the Hugoniot curve describes an Euler shock. This fact is also shown in Fig. 4.

4.2.2 Slow Hugoniot locus

If for the Mach number

$$M_0 \to \hat{c}_s^{(0)}(A, B) = \frac{c_s|_0}{a_0} \tag{51}$$

holds, a slow shock becomes possible. The slow Hugoniot locus is more involved than that of the fast family. First of all the Mach number turned out to be not a practical pathvariable, since it varies non-monotonically along the locus. Unfortunately all the familiar quantities, like transversal field, pressure or density, behave in a non-monotone manner. Thus in the calculations the pathvariable is changed appropriately when tracing the Hugoniot locus. In Appendix B explicit expressions for the fields behind a slow shock are given.

The slow Hugoniot locus at constant A for different values of B is depicted in Fig. 5. Again the values of magnetic field, pressure and specific volume are shown. Along the

x-axis varies the Mach number. Note, that for certain Mach numbers two possible shock solutions exist. This fact corresponds to the non-convexity of the MHD equations. Furthermore the interval for the Mach number of a slow shock is finite. There exist Mach numbers such that no slow shock is possible. Of course, this follows already from the non-monotonicity of M_0. The end of a slow Hugoniot locus is always given by a rotational wave in which the transversal magnetic field is rotated by an angle of π.

The limiting behavior of the slow Hugoniot locus is not very clear. From Fig. 5 one may read off that for $B \to 0$ the slow Hugoniot locus vanishes. In the case $A \to 0$ the cases $B^2 \lessgtr \gamma$ have to be distinguished. Numerical evaluations suggest that for $B^2 < \gamma$ the locus vanishes whereas for $B^2 > \gamma$ it approaches the Hugoniot locus of the Euler equations. Investigations like in [8]/[9] might bring more insight into this field.

4.2.3 Non-regularity

The shocks realized along the *fast* Hugoniot curve of Fig. 4 always have a regular characteristic behavior. They form classical Lax shocks. The slow Hugoniot locus, however, is decomposed into segments of different non-regular behavior. In the following this non-regularity is discussed. The nomenclature referrs to Fig. 6 as well as to the common 1-2-3-4 notation introduced by [15]. In the 1-2-3-4 notation the regular slow and fast shocks are 3-4 and 1-2 shocks, whereas 1-3, 1-4, 2-3 and 2-4 shocks form intermediate waves.

The transversal magnetic field is decreased across a slow shock. As far as the transversal field stays away from zero behind the shock, the shock forms a Lax shock (3-4 shock). The characteristics in front and behind of such a shock are sketched in the lower right corner of Fig. 5. If the transversal field passes zero, an intermediate shock arises with non-regular characteristic behavior. In Fig. 6 the transversal magnetic field of three slow Hugoniot loci is shown and the non-regular segments are indicated. There are two different single overcompressive shocks in which one additional characteristic points into the shock. They are denoted by C^+ which corresponds to a 2-4 intermediate shock and by $\tilde{\mathsf{C}}^+$ which corresponds to a 1-3 intermediate shock. C^{++} (1-4 intermediate) denotes a double overcompressive shock with two additional characteristics pointing into the shock. The so-called Alfven-shock is denoted by A and describes a 2-3 intermediate shock. A Alfven-shock looks like a Lax shock, but for the linear degenerated field associated to the eigenvalue $v \pm c_A$. The different scenarios of the characteristics of the intermediate shocks may be read off Fig. 7. It is interesting to remark, that 1-3 and 1-4 shocks intuitively could be considered as *fast* shocks. However, they appear while tracing the slow Hugoniot locus.

Note that the Hugoniot locus in Fig. 6 shows the transition between the different intermediate shocks very clearly. Once the transversal field becomes negative, the inflow velocity (referring to the picture of a stationary shock) reaches the Alfven velocity. Depending of the choice of the parameter A and B it might even happen, that the inflow becomes super-fast. At this point the Alfven and fast characteristic in front of the shock has turned into it (first C^+ and then C^{++}). The maximal value of the inflow velocity M_0 is reached, if the slow characteristic behind the shock is parallel to it. By tracing the Hugoniot locus further this characteristic points out of the shock (A, resp. $\tilde{\mathsf{C}}^+$). By and by the fast and Alfven characteristic in front of the shock again turn out of the shock, while the inflow velocity again drops below the fast velocity and aproaches the Alfven velocity. At the end of the Hugoniot locus the Alfven-shock becomes a rotational wave with both Alfven characteristics in front and behind the shock parallel to it.

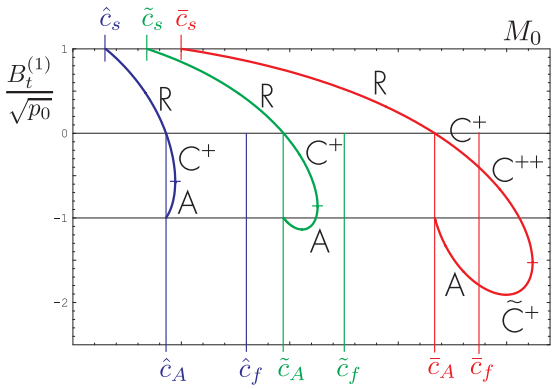

Figure 6: Indication of the non-regular sections along three different slow Hugoniot loci. As example, the transversal magnetic field is shown. The non-regular shocks are intermediate shocks in which the transversal magnetic field changes sign. The shock changes type if the Mach number of the inflow reaches the different characteristic velocities. Note, that the velocities $\hat{c}$, $\tilde{c}$ and $\bar{c}$ referr to the different Hugoniot loci shown, i.e. they belong to different values of the parameter B.

In the MHD system also compound waves may occur. In such a wave a slow rarefaction is directly attached to a slow shock. The slow shock travels with its maximal propagation speed. The slow characteristic in the back of the shock is then parallel to the shock and gives way to the rarefaction.

It has been mentioned in the introduction that the relevance and physical significance of intermediate shocks is lively discussed. A very strong result [5] shows the stability of intermediate shocks in a 3d numerical simulation under finite perturbations. Theoretically they are shown [16], [17] to be stable according to a nonlinear stability analysis. It seems that intermediate waves may not yet be abondoned in MHD investigations.

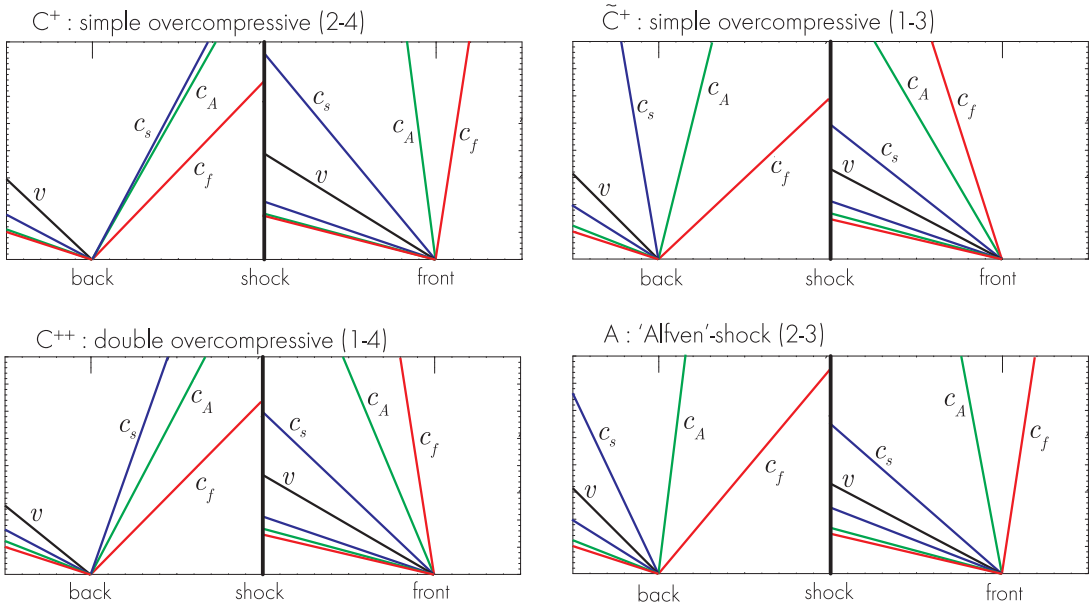

Figure 7: Characteristic curves in front and in the back of non-regular waves occuring along the slow Hugoniot locus shown in Fig. 6. The shock is viewed stationary as vertical line in the middle of the pictures.

5 Controlling the rarefaction waves

The fast and slow characteristic family allow expansion of the plasma by rarefaction waves. The admissible states are described by the integral curves of the eigenvectors of the Jacobian of the fluxfunction in (8).

Along the integral curves the primitive variables

$$\varphi = (\rho, v_n, \mathbf{v}_t, \mathbf{B}_t, p) \tag{52}$$

are used. From the eigenvectors (see e.g. [3]) follows that like in the case of a shock wave only the absolute value of the transversal magnetic field may change. The equations of the integral curves may be integrated in the case of the density and the pressure to give

$$\begin{aligned} \rho(s) &= \rho_0\, e^{-s} \\ p(s) &= p_0\, e^{-\gamma s} \end{aligned} \tag{53}$$

The remaining fields are described by the ordinary differential equations

$$\begin{aligned} v_n'(s) &= \mp c_{s,f}(s) \\ \mathbf{v}_t'(s) &= \frac{\mp c_{s,f}(s)}{\left(\frac{c_A(s)}{c_{s,f}(s)}\right)^2 - 1} \frac{\mathbf{B}_t(s)}{B_n} \\ B_t'(s) &= \frac{B_t(s)}{\left(\frac{c_A(s)}{c_{s,f}(s)}\right)^2 - 1}. \end{aligned} \tag{54}$$

The curve is parametrized by $s > 0$. Note that the fast, slow and Alfven velocity $c_{s,f,A}$ defined in (9) depend on the values of density pressure and magnetic field and thus on s along the integral curve. The $+$-sign ($-$-sign) belongs to a left (right) going rarefaction wave.

It may be read off (54) that in contrast to the fast and slow shock wave the transversal magnetic field always decreases in a fast rarefaction and increases in a slow one. The fast integral curve ends if B_t vanishes. Thus there is a maximal value of s given by

$$B_t(s^{(\max)}) = 0. \tag{55}$$

where $B_t(s)$ is the solution of (54). Of course, the value of $s^{(\max)}$ depends on the initial conditions at the starting point of the rarefaction.

The system (54) may not be solved analytically. In the implementation of a Riemann solver the ordinary differential equations are solved numerically in order to describe rarefaction waves.

6 Implementation

The algebraic system which have to be solved in order to solve the Riemann problem is given in (21) together with (23). It only remains to define pathvariables $\psi_{f,s}$ for the fast and slow wave. In the implementation both pathvariables should be $\in \mathbb{R}$ to aviod problems at artificial boundaries. Positive values will represent shocks, negative values correspond to rarefactions.

The fast family is rather straight forward to parametrized. This paper suggests

$$\psi_f > 0 \quad \text{fast shock with velocity } v_s = c_f^{(loc)} + \psi_f \tag{56}$$

$$\psi_f < 0 \quad \text{fast rarefaction of strength } s_{end} = s^{(\max)} \tanh\left(-\psi_f\right). \tag{57}$$

where $c_f^{(loc)}$ is the fast velocity calculated with the local fields in front of the shock. Thus the fast shock is described by its propagation speed relative to the fast velocity. For a fast rarefaction, $\psi_f \in \mathbb{R}$ is transformed to the valid interval $\left(0, s^{(\max)}\right)$ of the integration variable s.

The slow waves may be described by

$$0 < \psi_s \leq \hat{B}_t^{(\star)} \quad \text{slow shock with } \left.\hat{B}_t\right|_1 = A - \psi_s \tag{58}$$

$$\psi_s > \hat{B}_t^{(\star)} \quad \text{slow shock with } \hat{B}_t^{(\star)} + \text{rarefaction with } s_{end} = \psi_s - \hat{B}_t^{(\star)} \tag{59}$$

$$\psi_s < 0 \quad \text{slow rarefaction with } s_{end} = -\psi_s \tag{60}$$

Here the shock interval $\psi_s > 0$ is splitted into two parts. The first part describes a slow shock where ψ_s is the jump in the transversal magnetic field $\hat{B}_t$ (locally dimensionless). The second part corresponds to a compound wave in which a slow rarefaction is attached to a slow shock with maximal Mach number $M_0^{(\max)}$. The single shock is only considered up to the value $\psi_s = \hat{B}_t^{(\star)}$ at which the maximal Mach number is reached, see Appendix B for details. The slow rarefaction, either pure or in a compound wave, is described by the integration variable s.

Note, that the pathvariable (58)-(60) pays full attention to non-regular 2-4 and 1-4 shocks, but not to Alfven shocks (2-3) and $\tilde{C}^+$-shocks (1-3). These waves are in a way substituted by the compound wave. Compound waves are well known in numerical MHD simulations, whereas the Alfven-shock, for instance, as shock in a linear family rather needs further investigations. Until the relevance of such shocks is not clarified, the definitions (58)-(60) should be considered as a first empirical approach to the implementation of a MHD Riemann solver.

In the present implementation the system (21) is solved by the classical method of Newton. The Jacobian of RP is calculated by finite differences. The ODE system (54) is solved by a explicit Runge-Kutta-method (see [10]). For solving (73) in the case of a fast shock also Newtons method has been applied. The simple Newton method is known to be sensitive with respect to the initial guess. The present implementation worked satisfactory, though, in some cases, special care had to be taken for the initial guess.

6.1 Results

As concluding result the exact solution of the Riemann problem given by the initial conditions (18)/(19) is presented. In Table 1 and 2 the values of the fields are given together with the positions of the waves. The tables have to be read from left to right and the columns give the values *behind* the corresponding wave. If the wave does not change a quantity the entry is left out. The graphs of the fields have been depicted in Fig. 2.

For the solver the initial guess was chosen to be

$$\left(\psi_f^-, \psi_s^-, \alpha_R, \psi_s^+, \psi_f^+\right)_{\text{guess}} = (0.01, 0.01, 0.01, 0.01, 0.01)\,. \tag{61}$$

	state 1	fast raref.	rotation	slow raref.
x_{start}		-1.474922	-0.631585	-0.521395
x_{end}		-0.990247	./.	-0.445268
ρ	3.000000	2.340949		2.200167
v_x	0.000000	0.348797		0.402052
v_y	0.000000	-0.144157	-0.339270	0.286284
v_z	0.000000	0.000000	0.354780	0.438321
B_y	1.000000	0.642777	0.344252	0.413199
B_z	0.000000	0.000000	0.542820	0.651535
p	3.000000	1.984139		1.789281

Table 1: Results for the initial data (18)/(19). The table shows the values of the fields and the positions of the waves in the negative halfspace. It is continued by Table 2.

	contact	slow shock	rotation	fast shock
x_{start}	0.402052	1.279598	1.568067	2.072332
x_{end}	./.	./.	./.	./.
ρ	1.408739	1.054703		1.000000
v_x		0.107484		0.000000
v_y		-0.514217	-0.006260	0.000000
v_z		0.078923	-0.088275	0.000000
B_y		0.601050	0.079386	$\cos(0.5)$
B_z		0.947741	1.119452	$\sin(0.5)$
p		1.093004		1.000000

Table 2: Results for the initial data (18)/(19). This table continues Table 1 and shows the values of the fields as well as the wave positions in the positive halfspace.

In Table 3 the convergence behavior of the Newton method is shown. The solver proceeds with quadratic convergence within the last 3 iterations. The residual drops below 10^{-9}. The quadratic convergence of the solver has been observed over a wide range of initial conditions. For the solution of the system (21)

$$\begin{aligned}&\left(\psi_f^-, \psi_s^-, \alpha_R, \psi_s^+, \psi_f^+\right)_{\text{solution}}\\ &= (-0.451045, -0.062023, 1.005614, 0.335496, 0.061318)\end{aligned} \tag{62}$$

is calculated. From this it may be read off immediately that both waves to the left are rarefactions, since $\psi_{s,f}^- < 0$. Analogously, both waves to the right are shocks.

The results in Table 1 and 2 now could be used as benchmark for numerical schemes for magnetohydrodynamics. The will be done in a future paper.

Iteration	Residual $\left\|\mathrm{RP}_U(\Psi)\right\|_\infty$
0	2.0521587682
1	0.8758019116
2	0.1715716821
3	0.0093181931
4	0.0000548088
5	0.0000000007

Table 3: Iteration vs. residual during the solution of the Riemann problem given by (18)/(19). The initial guess may be read off (61).

7 Uniqueness conditions

If a hyperbolic system is strictly hyperbolic and each characteristic family is either genuine non-linear or linearly degenerated, then the theorem of Lax ([13], [18]) gives local existence and uniqueness to the Riemann problem. Clearly the requirements of the theorem are not given in the case of MHD. However, if we characterise the transversal magnetic field by polar coordinates with *positiv* absolute value and *neglect the non-regular part* of the slow Hugoniot locus, we match the conditions. The slow and the fast family then form genuinely non-linear fields and the characteristic and shock velocities stay apart. By this setting, the whole phase space of the variables (6) may be acquired by *regular* Hugoniot curves and integral curves. Thus it seems suggestive that, by virtue of Lax' theorem, there exists exactly one *regular* solution of a MHD Riemann problem. Based on this argumentation it will be assumed that in a non-unique solution of the Riemann problem only non-regular solutions are added.

The main ingredient to derive uniqueness conditions is the following: If a non-regular wave is inserted at one side of the solution, the Alfven wave at this side disappears, since the non-regular wave skips the Alfven characteristic. The Alfven waves, however, are the only waves that could change the directions of the transversal magnetic field. Even the non-regular wave changes only the absolute value. Thus, if a non-regular wave is inserted at *each* side, only planar initial conditions will be met. If only one non-regular wave is present, non-planar initial data could be met, provided the remaining rotational wave will adjust exactly the twist angle of the initial conditions. This fixes the rotation angle a priori by the initial conditions. Hence, one degree of freedom in (24) is missing and one variable of the initial conditions may not be prescribed, but follow from the non-regular solution. It will be shown that the following condition is sufficient:

Uniqueness condition 1 *If for the initial conditions in the non-planar case the condition* $[[\mathbf{v}_t]]_{initial} = 0$, *or in the coplanar case the condition* $0 \neq [[\mathbf{v}_t]]_{initial} \nparallel [[\mathbf{B}_t]]_{initial}$ *holds, then the MHD Riemann problem has an unique regular solution.*

It follows, for instance, that the solution of (18)/(19) depicted in Fig. 2 is unique, since $\mathbf{v}_t \equiv 0$ initially. To derive this condition we proceed as follows:

In the initial conditions of a MHD Riemann problem we are free to choose the coordinate axes for the magnetic field and the Galilei-frame for the velocity. Therefore any non-planar initial data may be brought into the form

$$\mathbf{v}_t^{(1)} = \mathbf{0} \qquad \mathbf{B}_t^{(1)} = \begin{pmatrix} B_t^{(1)} \\ 0 \end{pmatrix} \tag{63}$$

$$\mathbf{v}_t^{(0)} = \begin{pmatrix} v_y \\ v_z \end{pmatrix} \qquad \mathbf{B}_t^{(0)} = B_t^{(0)} \begin{pmatrix} \cos\alpha \\ \sin\alpha \end{pmatrix} \quad \alpha \neq 0 \tag{64}$$

with positive transversal field $B_t^{(0)/(1)} > 0$. The case of initially vanishing transversal field is not considered. The (1)- and (0)-state shall be chosen such that the non-regular wave is inserted at the (1)-side of the initial conditions. In Fig. 8 the situation and notation is sketched. Note, that all waves between state (1) and state ($\star$) change only the absolute value of $\mathbf{B}_t$. Additionally, in any wave of MHD Riemann problems the transversal velocity is connected to the transversal magnetic field by

$$[[\mathbf{v}_t]] = C\ [[\mathbf{B}_t]] \tag{65}$$

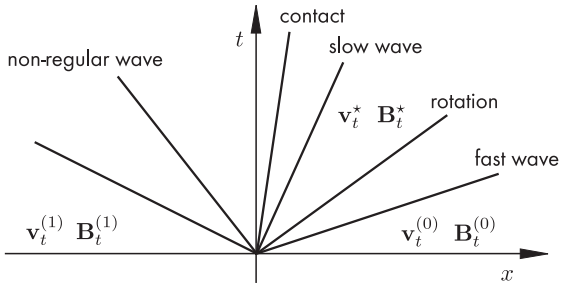

Figure 8: Settings and notations referring to the initial conditions (63)/(64) and equation (67).

where the constant C differs for the different waves. Starting from the left hand side (1) and inserting waves towards the (0)-side, it follows that the transversal velocity and magnetic field in the back of the right going rotational wave will have the form

$$\mathbf{v}_t^\star = \begin{pmatrix} a \\ 0 \end{pmatrix} \qquad \mathbf{B}_t^\star = \begin{pmatrix} B_t^\star \\ 0 \end{pmatrix} \tag{66}$$

with some constant $a \neq 0$. We now look at the Alfven and fast wave that travel to the right. If the non-regular solution exists, the equation

$$\mathbf{v}_t^\star = \mathbf{v}_t^{(0)} + C_f \; [[\mathbf{B}_t]]_f + C_A \; [[\mathbf{B}_t]]_A \tag{67}$$

must hold. In Appendix C is shown that this equation implies

$$v_z = \Lambda \sin\alpha \qquad \text{with } \Lambda \neq 0 \tag{68}$$

Therefore, a non-planar Riemann problem with $v_z = 0$ has no non-regular solution. The above stated condition follows in the case of general initial conditions.

The constant Λ depends on the solution and thus on the initial conditions of the remaining variables. In fact, (68) forms a constraint to the initial conditions if a non-regular solution is required. The investigation of this condition and its physical relevance is subject to future work.

A Details for the fast shock

¿From the equations in (43) follow the Hugoniot curve and the Rayleigh line

$$\hat{p}_R\left(\hat{v},\hat{B}_t,M_0,A\right)=1-\gamma M_0^2\left(\hat{v}-1\right)-\tfrac{1}{2}\left(\hat{B}_t^2-A^2\right) \tag{69}$$

$$\hat{p}_H\left(\hat{v},\hat{B}_t,A\right)=\frac{\hat{v}-\frac{\gamma+1}{\gamma-1}+\frac{1}{2}\left(\hat{v}-1\right)\left(A-\hat{B}_t\right)^2}{1-\frac{\gamma+1}{\gamma-1}\hat{v}} \tag{70}$$

which after substitution of $\hat{B}_t$ by

$$\hat{B}_t\left(\hat{v},M_0,A,B\right)=A\frac{\gamma M_0^2-B^2}{\gamma M_0^2\,\hat{v}-B^2} \tag{71}$$

form pure functions of the specific volume and the parameter M_0, A and B. The intersections of $\hat{p}_R(\hat{v})$ and $\hat{p}_H(\hat{v})$ in the $(\hat{p},\hat{v})$-plane represent the solutions of the Rankine-Hugoniot-conditions. If we define

$$\hat{v}^{(\min)}\left(M_0,B\right)=\begin{cases}\frac{\gamma-1}{\gamma+1} & \frac{B^2}{\gamma M_0^2}<\frac{\gamma-1}{\gamma+1}\\ \frac{B^2}{\gamma M_0^2} & \frac{B^2}{\gamma M_0^2}>\frac{\gamma-1}{\gamma+1}\end{cases} \tag{72}$$

then for $M_0>\hat{c}_f^{(0)}$ there exists exactly one intersection of $\hat{p}_R\left(\hat{v}\right)$ and $\hat{p}_H\left(v\right)$ in the interval $(\hat{v}^{(\min)},1)$. This intersection corresponds to a fast shock. The other intersections (if they exist) lay at the branch of $\hat{p}_R(\hat{v})$ with $\hat{v}<B^2/(\gamma M_0^2)$ and correspond to a (1-3) and (1-4) shock. The equation

$$\hat{p}_R\left(\hat{v},\hat{B}_t\left(\hat{v},M_0,A,B\right),M_0,A\right)=\hat{p}_H\left(\hat{v},\hat{B}_t\left(\hat{v},M_0,A,B\right),A\right) \tag{73}$$

is cubic in $\hat{v}$ and has to be solved numerically. Pressure $\hat{p}$ and magnetic field $\hat{B}_t$ follow then from $\hat{v}$. In the case $B=0$ from (73) follows a quadratic equation for $\hat{v}$ with one solution $\hat{v}>0$ that reads

$$\hat{v}\left(M_0,A\right)=\frac{\left(\gamma-1\right)M_0^2+A^2+2}{2\left(\gamma+1\right)M_0^2}+\sqrt{\left(\frac{\left(\gamma-1\right)M_0^2+A^2+2}{2\left(\gamma+1\right)M_0^2}\right)^2+\frac{2-\gamma}{\gamma\left(\gamma+1\right)M_0^2}A^2}. \tag{74}$$

In the limiting case of $A=0$ there exists a "switch-on" shock with $\hat{B}_t^{(1)}\neq 0$ if (50) and $B^2>\gamma$ hold. The transversal magnetic field is then given by

$$\hat{B}_t\left(M_0,B\right)=\sqrt{\frac{\gamma M_0^2-B^2}{B^2}\left(\left(\gamma-1\right)\left(\tfrac{\gamma+1}{\gamma-1}B^2-\gamma M_0^2\right)-2\gamma\right)} \tag{75}$$

and the specific volume follows from

$$\hat{v}\left(M_0,B\right)=\frac{B^2}{\gamma M_0^2} \tag{76}$$

If a "switch-on" shock is not admissible an ordinary Euler shock with

$$\hat{v}\left(M_0\right)=\frac{\left(\gamma-1\right)M_0^2+2}{\left(\gamma+1\right)M_0^2} \tag{77}$$

is realized.

B Details for the slow shock

To calculate a slow shock the transversal magnetic field will be used as parameter in (69) and (70), whereas the Mach number will be eliminated via

$$M_0\left(\hat{v},\hat{B}_t,A,B\right)=\sqrt{\frac{B^2}{\gamma}\frac{\hat{B}_t-A}{\hat{B}_t\hat{v}-A}} \tag{78}$$

It follows the quadratic equation

$$a\left(\hat{B}_t,A,B\right)\,\hat{v}^2+b\left(\hat{B}_t,A,B\right)\,\hat{v}+c\left(\hat{B}_t,A,B\right)=0 \tag{79}$$

for the specific volume, where the coefficients read

$$a\left(\hat{B}_t,A,B\right)=\frac{\hat{B}_t}{2}\left(4\tfrac{\gamma}{\gamma-1}+\left(\hat{B}_t-A\right)^2+\tfrac{\gamma+1}{\gamma-1}\left(A^2-\hat{B}_t^2\right)\right)-\tfrac{\gamma+1}{\gamma-1}B^2\left(\hat{B}_t-A\right) \tag{80}$$

$$b\left(\hat{B}_t,A,B\right)=\tfrac{\gamma}{\gamma-1}\left(A\left(\hat{B}_t^2-A^2\right)+2B^2\left(\hat{B}_t-A\right)-2\left(\hat{B}_t+A\right)\right) \tag{81}$$

$$c\left(\hat{B}_t,A,B\right)=\tfrac{2\gamma}{\gamma-1}A-\left(A^2+B^2\right)\left(\hat{B}_t-A\right). \tag{82}$$

Both solutions

$$\hat{v}^{\pm}\left(\hat{B}_t,A,B\right)=-\frac{1}{2a}\left(b\pm\sqrt{b^2-4ac}\right) \tag{83}$$

play a role along the slow Hugoniot locus. First only $\hat{v}^+$ lies in the valid range $(\frac{\gamma+1}{\gamma-1},1)$. The second solution $\hat{v}^-$ becomes smaller than one if $\hat{B}_t<-A$ is reached. Both solutions join at a minimal value of $\hat{B}_t$ which is given by

$$\hat{B}_t^-\left(A,B\right)=-\frac{4(B^2-\gamma)^2+\gamma^2A^4+4A^2(B^2+\gamma^2)}{2\gamma AB^2+\gamma\left(2-\gamma\right)A\left(2+A^2\right)+4B\sqrt{\left(\gamma-1\right)\Delta\left(A,B\right)}} \tag{84}$$

with the abbreviation

$$\Delta\left(A,B\right):=\left(B^2-\gamma\right)^2+A^2\tfrac{\gamma\left(\gamma^2-2\gamma+2\right)}{\gamma-1}+A^2\left(2B^2+A^2\right). \tag{85}$$

Given the transversal field (like in (58)) the specific volume follows from (83). The value of the pressure and the Mach number of the shock may be calculated from (69) and (78), respectively.

The maximal Mach number of a slow shock is given by the following relations. In a slow shock with maximal propagation velocity the normal velocity behind the shock equals the slow characteristic velocity. For the corresponding transversal magnetic field $B_t^{(\star)}$ follows the equation

$$\hat{v}^{(\star)}M_0\left(\hat{v}^{(\star)},\hat{B}_t^{(\star)},A,B\right)=\hat{c}_s^{(1)}\left(\hat{v}^{(\star)},\hat{p}^{(\star)},\hat{B}_t^{(\star)},A,B\right) \tag{86}$$

$$\text{with}\quad \hat{v}^{(\star)}=\hat{v}^+\left(\hat{B}_t^{(\star)},A,B\right),\quad \hat{p}^{(\star)}=\hat{p}_R\left(\hat{v}^+\left(\hat{B}_t^{(\star)},A,B\right),\hat{B}_t^{(\star)},M_0,A\right) \tag{87}$$

and the maximal Mach number is then given by

$$M_0^{(\max)}=M_0\left(\hat{v}^{(\star)},\hat{B}_t^{(\star)},A,B\right). \tag{88}$$

C Uniqueness argument

The Alfven wave changes only the direction, whereas the fast wave changes the absolute value. Hence, from (67) follows

$$\mathbf{v}_t^\star = \mathbf{v}_t^{(1)} + C_f\ [[\mathbf{B}_t]]_f + C_A\ [[\mathbf{B}_t]]_A \tag{89}$$

$$= \begin{pmatrix} v_y \\ v_z \end{pmatrix} + C_f \left(B_t^\star - B_t^{(0)}\right) \begin{pmatrix} \cos\alpha \\ \sin\alpha \end{pmatrix} + C_A \left(\begin{pmatrix} B_t^\star \\ 0 \end{pmatrix} - B_t^\star \begin{pmatrix} \cos\alpha \\ \sin\alpha \end{pmatrix} \right) \tag{90}$$

and, with knowledge of $\mathbf{v}_t^\star = (a, 0)$,

$$\begin{pmatrix} v_y \\ v_z \end{pmatrix} \stackrel{!}{=} \begin{pmatrix} a - C_A B_t^\star + \left(C_A B_t^\star - C_f \left(B_t^\star - B_t^{(0)}\right)\right)\cos\alpha \\ \left(C_A B_t^\star - C_f \left(B_t^\star - B_t^{(0)}\right)\right)\sin\alpha \end{pmatrix}. \tag{91}$$

This equation has to hold in the case of a non-regular solution. It will now be shown that

$$C_A B_t^\star - C_f \left(B_t^\star - B_t^{(0)}\right) \neq 0 \tag{92}$$

holds. The coefficients C_A and C_f depend on the fields in the solution, but have the same sign, see (40), (46) and (54). From the initial conditions we have $B_t^\star > 0$ and $B_t^{(0)} > 0$. In the case of the fast wave being a rarefaction, the transversal magnetic field is decreased

$$B_t^\star < B_t^{(0)} \tag{93}$$

and thus (92) is true. On the other hand, in the case of a shock it may be shown that

$$\left(\frac{C_A}{C_f} - 1\right) B_t^\star + B_t^{(0)} \neq 0 \tag{94}$$

is true. In order to do so, we proof

$$\frac{C_A}{C_f} > 1. \tag{95}$$

¿From (40) follows $C_A = \pm 1/\sqrt{\gamma\hat{\rho}^\star}$ in the case of dimensionless variables according to (42). Together with (46) the inequality (95) is equivalent to

$$\hat{v}^\star > \frac{B^2}{\gamma M_0^2} \tag{96}$$

which is true since, see (71),

$$\hat{v}^\star = \frac{B^2}{\gamma M_0^2} + \frac{A}{B_t^\star}\left(1 - \frac{B^2}{\gamma M_0^2}\right) > \frac{B^2}{\gamma M_0^2} \tag{97}$$

with $M_0^2 > B^2/\gamma$ for a fast shock. Therefore in any case the transversal velocity component v_z is given in the form (68) in a non-regular solution.

References

[1] J. Bazer and W. B. Ericson, *Hydromagnetic Shocks*, Astrophys. J. **129** (1958) p.758

[2] A. A. Barmin, A. G. Kulikovskiy, and N. V. Pogorelov, *Shock-Capturing Approach and Nonevolutionary Solutions in Magnetohydrodynamics*, J. Comp. Phys. **126** (1996) p.77

[3] M. Brio and C. C. Wu, *An Upwind Differencing Scheme for the Equations of ideal Magnetohydrodynamics*, J. Comp. Phys. **75** (1988) p.400

[4] H. DeSterck and S. Poedts, *Intermediate Shocks in Three-Dimensional Magnetohydrodynamic Bow-shock Flows with Multiple Interacting Shock Fronts*, Phys. Rev. Let. **84**/24 (2000) p.5524

[5] H. DeSterck and S. Poedts, *Disintegration and reformation of intermediate shock segments in three-dimensional MHD bow shock flows*, to appear in J. Geophys. Res.

[6] W.B.Ericson and J.Bazer, *On Certain Properties of Hydromagnetic Shocks*, Phys. Fluids **3**/4 (1960) p.631

[7] S. A. E. G. Falle and S. S. Komissarov, *On the Inadmissibility of Non-evolutionary Shocks*, J. Plasma Phys. **65** (2001) p.29

[8] H. Freistühler and P. Szmolyan, *Existence and Bifurcation of Viscous Profiles for All Intermediate Magnetohydrodynamic Shock Waves,* SIAM J. Math. Anal. **26**/1 (1995) p.112

[9] H. Freistühler and C. Rohde, *Numerical Methods for Viscous Profiles of Non-classical Shock Waves*, Proc. 7th Intl. Conf. Hyp. Problems, Intl. Series of Num. Math. (vol.129), Birkhäuser Verlag (1999)

[10] E. Hairer, S. P. Nørsett, and G. Wanner, *Solving ordinary differential equations I* (2nd edn), Springer series in comp. math. (vol. 14), Springer Verlag, Berlin (1993)

[11] A. Jeffrey and T. Taniuti, *Non-linear Wave Propagation*, Academy Press, New York (1964)

[12] L. D. Landau and E. M. Lifshitz, *Electrodynamic of Continuous Media*, Course in theoretical physics (vol. 8), Pergamon Press, Oxford (1960)

[13] P. D. Lax, *Hyperbolic Systems of Conservation Laws II*, Comm. Pure Appl. Math. **10** (1957) p.537

[14] R. J. LeVeque, *Numerical Methods for Conservation Laws* (2nd edn), Lectures in Mathematics, Birkhäuser Verlag, Basel (1992)

[15] M. A. Liberman and A. L. Velikovich, *Physics of Shock Waves in Gases and Plasmas*, Springer Series in Electrophysics (vol.19), Springer, Berlin (1986)

[16] R. S. Myong and P. L. Roe, *Shock Waves and Rarefaction Waves in Magnetohydrodynamics. Part 1. A Model System*, J. Plasma Phys. **58**/3 (1997) p.485

[17] R. S. Myong and P. L. Roe, *Shock Waves and Rarefaction Waves in Magnetohydrodynamics. Part 2. The MHD System*, J.Plasma Phys. **58**/3 (1997) p.521

[18] D. Serre, *Systems of Conservation Laws* (vol. 1), Cambridge Univ. Press, Cambridge (1999)

[19] E. F. Toro, *Riemann Solvers and Numerical Methods for Fluid Dynamics* (2nd edn), Springer, Berlin (1999)

[20] C. C. Wu, *Formation, Structure, and Stability of MHD Intermediate Shocks*, J. Geophys. Res. (space physics) **95**/6 (1990) p.8149

[21] C. C. Wu, *Magnetohydrodynamic Riemann Problem and the Structure of the Magnetic Reconnection Layer*, J. Geophys. Res. (space physics) **100**/4 (1995) p.5579

Research Reports

No.	Authors	Title
02-06	M. Torrilhon	Exact Solver and Uniqueness Conditions for Riemann Problems of Ideal Magnetohydrodynamics
02-05	C. Schwab, R.-A. Todor	Sparse Finite Elements for Elliptic Problems with Stochastic Data
02-04	R. Jeltsch, K. Nipp	CSE Program at ETH Zurich: Are we doing the right thing?
02-03	L. Diening, A. Prohl, M. Ruzicka	On Time-Discretizations for Generalized Newtonian Fluids
02-02	A. Toselli	*hp* Discontinuous Galerkin Approximation for the Stokes Problem
02-01	F.M. Buchmann, W.P. Petersen	Solving Dirichlet problems numerically using the Feynman-Kac representation
01-09	A.-M. Matache	Sparse Two-Scale FEM for Homogenization Problems
01-08	C. Lasser, A. Toselli	Convergence of some two-level overlapping domain decomposition preconditioners with smoothed aggregation coarse space
01-07	T. von Petersdorff, C. Schwab	Wavelet-discretizations of parabolic integro-differential equations
01-06	A.-M. Matache, C. Schwab	Two-Scale FEM for Homogenization Problems
01-05	A. Buffa, R. Hiptmair, T. von Petersdorff, C. Schwab	Boundary Element Methods for Maxwell Equations in Lipschitz Domains
01-04	R. Hiptmair, C. Schwab	Natural BEM for the Electric Field Integral Equation on polyhedra
01-03	C. Schwab, A.-M. Matache	Generalized FEM for Homogenization Problems
01-02	A. Toselli, C. Schwab	Mixed *hp*-finite element approximations on geometric edge and boundary layer meshes in three dimensions
01-01	A. Buffa, M. Costabel, C. Schwab	Boundary element methods for Maxwell's equations on non-smooth domains
00-18	B.Q. Guo, C. Schwab	Analytic regularity of Stokes flow in polygonal domains
00-17	M.H. Gutknecht, S. Röllin	Variations of Zhang's Lanczos-Type Product Method
00-16	M.H. Gutknecht, S. Röllin	The Chebyshev iteration revisited
00-15	G. Schmidlin, C. Schwab	Wavelet Galerkin BEM on unstructured meshes by aggregation